Chemical Engineering Science 119 (2014) 236–244

Contents lists available at ScienceDirect

Chemical Engineering Science

journal homepage: www.elsevier.com/locate/ces

Two-dimensional numerical study of flow dynamics of a nucleated cell tethered under shear flow

Zheng Yuan Luo [a,b,c], Long He [a,b], Shu Qi Wang [c], Savas Tasoglu [c,1], Feng Xu [b,d], Utkan Demirci [c,e,f,**], Bo Feng Bai [a,b,*]

[a] State Key Laboratory of Multiphase Flow in Power Engineering, Xi'an Jiaotong University, Xi'an 710049, PR China
[b] Bioinspired Engineering & Biomechanics Center, Xi'an Jiaotong University, Xi'an 710049, PR China
[c] Bio-Acoustic MEMS in Medicine (BAMM) Lab, Division of Biomedical Engineering and Division of Infectious Diseases, Department of Medicine, Brigham & Women's Hospital, Harvard Medical School, MA 02139, USA
[d] The Key Laboratory of Biomedical Information Engineering of Ministry of Education, School of Life Science and Technology, Xi'an Jiaotong University, Xi'an 710049, China
[e] Harvard-MIT Health Sciences and Technology, Cambridge, MA 02139, USA
[f] Department of Radiology, Stanford University School of Medicine, Canary Center for Early Cancer Detection, Palo Alto, CA 94304, USA

HIGHLIGHTS

- We developed a model to study the dynamics of a nucleated cell tethered under flow.
- Properties of nucleus significantly affect the flow dynamics of tethered cells.
- Presence of nucleus leads to leukocyte tether dynamics different from platelets.
- Varied internal viscosity leads to the variation in tether dynamics of leukocytes.

ARTICLE INFO

Article history:
Received 13 January 2014
Received in revised form
14 July 2014
Accepted 26 July 2014
Available online 1 August 2014

Keywords:
Biomedical engineering
Mathematical modeling
Multiphase flow
Cell tether
Cell capture/release
Microfluidics

ABSTRACT

When blood components (*e.g.*, leukocytes and platelets) adhere to a surface (*e.g.*, blood vessel wall), shear flow causes the elongation of the non-adherent part of the cell membrane forming a long thin cylinder shape (*i.e.*, cell tether). The formation of cell tether is important for regulation of cell adhesion strength and stabilization of cell rolling, and may significantly affect the flow dynamics inside the vessel, as well as the motion of other cells and bioactive molecules. Although significant efforts have been made to reveal mechanisms underlying cell tether formation, the role of nucleus, nucleus/cell volume ratio, nucleus/plasma viscosity ratio and cytoplasm/plasma viscosity ratio remains unknown. As such, we developed a two-dimensional mathematical model, in which leukocytes are regarded as compound viscoelastic capsules with a nucleus. We investigated the effects of several factors on flow dynamic characteristics of tethered cells, including the cell length, the inclination angle, the drag and lift forces acting on the cell. The presence of a nucleus (with nucleus/cell volume ratio of 0.44) led to a decrease of 33.8% in the cell length and an increase of 152%, 113% and 43.6% in the inclination angle, the drag force and lift force respectively compared to those of a cell without nucleus. For a cell with nucleus/cell volume ratio of 0.2, a 10-fold increase in cytoplasm/plasma viscosity ratio resulted in a decrease of 19.3% in the cell length and an increase of 93.9%, 155% and 131% in the inclination angle, the drag force and lift force respectively. These results indicate that nucleus and cytoplasm play a significant role in flow dynamics of nucleated cells tethered under shear flow. The developed mathematical model could be used to further understand the mechanisms of cell-adhesion related bioprocesses and to optimize the conditions for cell manipulation in microfluidics.

* Corresponding author at: State Key Laboratory of Multiphase Flow in Power Engineering, Xi'an Jiaotong University, Xi'an 710049, PR China. Tel.: +86 029 82665316; fax: +86 029 82669033.
** Co-corresponding author. Department of Radiology, Stanford University School of Medicine, Canary Center for Early Cancer Detection, Palo Alto, CA 94304, USA.
E-mail addresses: Utkan@stanford.edu (U. Demirci), bfbai@mail.xjtu.edu.cn (B.F. Bai).
[1] Present address: Department of Mechanical Engineering, University of Connecticut, 191 Auditorium Road, Unit 3139, Storrs, CT 06269-3139.

http://dx.doi.org/10.1016/j.ces.2014.07.048
0009-2509/

1. Introduction

When blood components adhere to a surface (*e.g.*, the wall of a blood vessel) and are subject to a flow at the same time, cell tethers (*i.e.*, long thin membrane cylinders extruded from adhered cells) may form due to the cooperation of hydrodynamic forces and adhesion forces. This phenomenon has been observed in *in vitro* experiments for different blood components. For example, leukocyte tethers with an average length of 5.9 μm (approximately radius of a leukocyte) were observed under physiological flow conditions (Schmidtke and Diamond, 2000), whereas platelet tethers with lengths of 3.2 – 16.6 μm (about 2 – 10 cell radii) were observed at a shear rate ranging from 150 to 10,000 s^{-1} (Dopheide et al., 2002). Cell tethers play an important role in cell adhesion related bioprocesses (*e.g.*, lymphocyte homing) and applications (*e.g.*, cell capture/release in microfluidic devices) (Tasoglu et al., 2013; Gurkan et al., 2012; Rizvi et al., 2013). For instance, dynamic alterations of cell tethers were revealed to stabilize leukocyte rolling (Ramachandran et al., 2004), which widely happens during lymphocyte homing. Cell tethers can also regulate cell adhesion strength, which may lead to flow-enhanced cell adhesion (Yago et al., 2007) and thus may affect the cell capture efficiency of microfluidic devices. Furthermore, numerous cell sorting applications (*e.g.*, sperm sorting) are strongly dependent on cell-microchannel wall interactions and potentially post-effects of adhered cells on flow dynamics inside channels (Tasoglu et al., 2013). However, the flow dynamics of tethered cells under shear flow are not yet completely clear, which has limited the understanding of cell adhesion related bioprocesses and applications.

Significant efforts have been contributed to understanding of tether formation and the flow dynamics of tethered cells under shear flow. A rigid microsphere model was firstly developed to study the formation of cell tethers under shear flow (King et al., 2005; Yu and Shao, 2007). A viscoelastic drop model (Khismatullin and Truskey, 2005) and an elastic capsule model (Berry et al., 2011) were further presented to incorporate dynamical cell deformation into tethered cell dynamics. However, some experimental observations were not discussed in these studies, *e.g.*, different cell tether lengths of leukocyte tethers and platelet tethers (Schmidtke and Diamond, 2000; Dopheide et al., 2002), large variations in leukocyte tether length ranging 1 – 25 μm (about 0.1 – 4-fold leukocyte radii) (Schmidtke and Diamond, 2000). The differences in size and morphology of leukocytes (spherical shape with a diameter of 10 – 20 μm) and platelets (discoidal shape with a diameter of 2 – 3 μm) were found to affect the adhesion dynamics (Berry et al., 2011). Another apparent difference between leukocyte and platelet is that a leukocyte has a nucleus but a platelet does not. In addition, mechanical properties of intracellular fluids, which were revealed to affect tether dynamics by *in vitro* experiments (Heinrich et al., 2005; Girdhar and Shao, 2007; Jauffred et al., 2007; Schmitz et al., 2008; Pospieszalska and Ley, 2009), may significantly vary even for the same types of cell, see Table 1. However, effects of these factors on the flow dynamics of tethered cells under shear flow are missing. Therefore, to develop a better understanding of tethered cell dynamics, further comprehensive investigations are required.

In this study, we developed a two-dimensional mathematical model to study the effects of several factors on the flow dynamics of tethered cells under shear flow. Among these factors are presence and absence of a nucleus, nucleus/cell volume ratio, nucleus/plasma viscosity ratio and cytoplasm/plasma viscosity ratio. Here, we developed a viscoelastic compound capsule model incorporating a nucleus, and evaluated hydrodynamic forces acting on the tethered cell. The results showed that the presence of a nucleus, nuclear and cytoplasmic properties significantly affected the flow dynamics of tethered cells under shear flow. These findings could explain experimental observations such as large variations in cell tether length and distinct characteristics of cell tethers between leukocytes and platelets. Our study provides new insights into tethered cell dynamics under shear flow, and the model presented here could be used to study functions of cell tethers in cell adhesion related bioprocesses, *e.g.*, regulating cell adhesion strength or stabilizing cell rolling.

2. Computational method

In Fig. 1, an initially spherical blood cell with radius R is tethered by a microvillus on cell membrane to the bottom plate. Computational domain extends approximately 12 drop radii in the x direction and 6 drop radii in the y direction. The cell is subject to a shear flow with an initial fluid velocity governed by a parabolic profile $\boldsymbol{u}^0=[ky(1-y/H), 0]$, which is a representative of the flow in a parallel-plate flow chamber. Here k is the bulk shear rate defined as $k=4u_{max}/H$, where u_{max} is the centerline velocity in the absence of cells. The blood cell (*e.g.*, leukocyte) with a nucleus is modeled as a compound viscoelastic capsule, which is a viscoelastic fluid including cytoplasm (density ρ_1 and viscosity μ_1) and nucleus (density ρ_2 and viscosity μ_2) surrounded by an elastic membrane (i.e., plasma membrane with shear modulus E_s). The cell without a nucleus (*e.g.*, platelet) is modeled as an elastic capsule, which is composed of a viscoelastic fluid with density ρ_1 and viscosity μ_1 surrounded by an elastic membrane with elastic modulus E_s. The

Table 1
Parameter values used in our computational model.

Parameter	Definition	Values	Reference
R (μm)	Cell radius	5	Bai et al. (2013), Luo et al. (2011b) and Geissmann et al. (2003)
L (μm)	Channel length	60	Bai et al. (2013) and Luo et al. (2011a, b)
H (μm)	Channel height	30	Stone and Kim (2001), Popel and Johnson (2005), Squires and Quake (2005), N'Dri et al. (2003) and Pappu et al. (2008)
k (s^{-1})	Shear rate	200–8000	Schmidtke and Diamond (2000), Dopheide et al. (2002) and Ramachandran et al. (2004)
ρ_0 (kg/m^3)	Density of plasma	1000	N'Dri et al. (2003), Khismatullin and Truskey (2004) and Berry et al. (2011)
μ_0 (mPa s)	Viscosity of plasma	1.0	N'Dri et al. (2003), Khismatullin and Truskey (2004) and Berry et al. (2011)
ρ_1 (kg/m^3)	Density of cytoplasm	1000	Bai et al. (2013) and Luo et al. (2011a, b)
$\lambda_{\mu 1}$	Cytoplasm/plasma viscosity ratio	500 – 5000	Schmid-Schonbein et al. (1980) and Khismatullin and Truskey (2004)
λ_1 (s)	Cytoplasmic relaxation time	0.176	Khismatullin and Truskey (2004)
α	Nuleus/cell volume ratio	0.2 – 0.44	Schmid-Schonbein et al. (1980), N'Dri et al. (2003) and Khismatullin and Truskey (2004)
ρ_2 (kg/m^3)	Nucleus density	1000	Khismatullin and Truskey (2004) and Bai et al. (2013)
$\lambda_{\mu 2}$	Nucleus/plasma viscosity ratio	5000 – 10,000	Schmid-Schonbein et al. (1980) and Khismatullin and Truskey (2004)
λ_2 (s)	Nuclear relaxation time	0.2	Khismatullin and Truskey (2004)
E_s (μN/m)	Elastic modulus of cell membrane	5 – 2500	Jadhav et al. (2005), Tasoglu et al. (2011, 2012) and Pappu et al. (2008)
k_b (μN/m)	Spring constant of adhesion bond	10,000	Khismatullin and Truskey (2004, 2005) and Luo et al. (2013)

cell is immersed in a Newtonian fluid (*e.g.*, plasma) with density ρ_0 and viscosity μ_0.

The incompressible Navier–Stokes equations governing the flow are given by

$$\nabla \cdot \mathbf{u} = 0 \tag{1}$$

$$\frac{\partial(\rho \mathbf{u})}{\partial t} + \nabla \cdot (\rho \mathbf{u}\mathbf{u}) = \nabla \cdot [-p\mathbf{I} + \mu_s(\nabla \mathbf{u} + \nabla \mathbf{u}^T) + \mathbf{T}_p] + \mathbf{F} \tag{2}$$

where ρ and t are the density and time respectively, $\mathbf{u}$ is the velocity vector, p and $\mathbf{I}$ are the pressure and unit tensor respectively, μ_s is the solvent viscosity (the Newtonian part of the viscoelastic fluid), and $\mathbf{F}$ is the body force from cell membrane. $\mathbf{T}_p$ is the viscoelastic stress from the non-Newtonian part of the viscoelastic fluid governed by the Oldroyd-B constitutive equation:

$$\lambda \left[\frac{\partial \mathbf{T}_p}{\partial t} + (\mathbf{u} \cdot \nabla)\mathbf{T}_p - \mathbf{T}_p \cdot (\nabla \mathbf{u}) - (\nabla \mathbf{u})^T \cdot \mathbf{T}_p \right] + \mathbf{T}_p = \mu_p [\nabla \mathbf{u} + (\nabla \mathbf{u})^T] \tag{3}$$

where μ_p and λ are the polymeric viscosity and relaxation time of the non-Newtonian part of the viscoelastic fluid respectively. The total viscosity of the viscoelastic fluid is the sum of the polymeric viscosity and solvent viscosity, *i.e.*, $\mu_1 = \mu_{p1} + \mu_{s1}$, $\mu_2 = \mu_{p2} + \mu_{s2}$.

Front tracking method is employed to capture the moving interface (*i.e.*, cell membrane) to consider elastic properties of cell membrane. In this method, the moving interface is tracked by Lagrangian points and is separated into many line segments in two-dimensional (2D) simulations. From the positions of Lagrangian points, the tension T_e in every line segment can be calculated as (Bagchi et al., 2005; Bagchi, 2007)

$$T_e = E_s(\varepsilon^{3/2} - \varepsilon^{-3/2}) \tag{4}$$

where ε is the undeformed length of a line segment divided by its deformed length. Instead of an accurate representation of cell membrane, the consideration of the complex internal structure of cells (*i.e.*, a nucleus in the cell) is central to this study. Thus, the classical Hooke's law is applied to the elastic membrane for its simplicity and ability to effectively capture the general features of elastic membranes (Jadhav et al., 2005; Barthes-Biesel et al., 2002). Then, the tension T_e in cell membrane can be distributed onto Eulerian grids as the body force term in Eq. (2) using the delta distribution function (Peskin, 1977; Unverdi and Tryggvason, 1992) as

$$D(x - x') = \begin{cases} \frac{1}{4h}\left[1 + \cos\left(\frac{\pi(x-x')}{2h}\right)\right] & \text{for} \quad |x - x'| \le 2h \\ 0 & \text{for} \quad |x - x'| > 2h \end{cases} \tag{5}$$

where x' is the position of a Lagrangian point on cell membrane and h is the Eulerian grid size. An indicator function $I(\boldsymbol{x},t)$ with value 2 inside nucleus, 1 inside cytoplasm and 0 outside the cell is defined and constructed from the known position of cell membrane. Fluid properties can thence be calculated by

$$\phi(\boldsymbol{x}, t) = \begin{cases} \phi_0 + (\phi_1 - \phi_0) I(\boldsymbol{x}, t), \text{for } I(\boldsymbol{x}, t) \le 1 \\ \phi_1 + (\phi_2 - \phi_1)(I(\boldsymbol{x}, t) - 1), \text{for } I(\boldsymbol{x}, t) > 1 \end{cases} \tag{6}$$

where ϕ represents fluid properties including ρ, μ_s, μ_p and λ. The indicator function is constructed by solving a Poisson equation (Unverdi and Tryggvason, 1992; Sarkar and Schowalter, 2000):

$$\nabla^2 I(\boldsymbol{x}, t) = \nabla \cdot \left[\sum_l D(\boldsymbol{x} - \boldsymbol{x}^{(l)}) \boldsymbol{n}^{(l)} \Delta s^{(l)} \right] \tag{7}$$

where $\boldsymbol{n}^{(l)}$, $\boldsymbol{x}^{(l)}$ and $\Delta s^{(l)}$ are the outward normal vector, centroid and length of a discrete line segment l of the membrane respectively. An Eulerian resolution of 40 grids for one cell diameter and a Lagrangian resolution of 250 elements for the cell membrane are used, which was identified to be sufficient in our previous work (Bai et al., 2013; Luo et al., 2013). Details of the method can be found in our previous studies (Bai et al., 2013; Luo et al., 2013) and articles by Tryggvason and co-workers (Unverdi and Tryggvason, 1992; Tryggvason et al., 2001; Tasoglu et al., 2008, 2010; Muradogluand and Tasoglu, 2010).

To simulate a tether, Berry et al. (2011) fixed a membrane point on the bottom plate, but they found that it may lead to numerical instability. In the adhesion dynamics of platelets and leukocytes, bonds are formed due to the receptor–ligand interactions. In the present study, a bond connecting the cell and bottom plate (Fig. 1a) is modeled as a spring. For the spring constant of the adhesion bond, a range of 500 – 10,000 μN/m was used in previous studies (Khismatullin and Truskey, 2004, 2005; Luo et al., 2013). Here, a large spring constant of 10,000 μN/m is used to ensure that the cell is not detached from the bottom plate. Besides, hydrodynamic forces $\boldsymbol{F}_{hy}$ acting on the tethered cell are calculated by

$$\mathbf{F}_{hy} = \int_C \mathbf{n} \cdot [-p\mathbf{I} + \mu_s(\nabla \mathbf{u} + \nabla \mathbf{u}^T) + \mathbf{T}_p] dl \tag{8}$$

where l denotes integration along cell membrane and $\mathbf{n}$ is the unit outward normal vector to the cell membrane. The hydrodynamic forces in 2D simulations include two components, *i.e.*, the drag force F_D in the flow direction and the lift force F_L perpendicular to the flow direction.

The governing equations are normalized by characteristic quantities, *e.g.*, characteristic velocity kR, length R, and time $1/k$. Dimensionless parameters include Reynolds number $Re = \rho_0 kR^2/\mu_0$, dimensionless membrane stiffness $G = \mu_0 kR/E_s$, Deborah number $De = \lambda k$, cytoplasm/plasma viscosity ratio $\lambda_{\mu 1} = \mu_1/\mu_0$, and nucleus/plasma viscosity ratio $\lambda_{\mu 2} = \mu_2/\mu_0$. Besides the drag force F_D and the lift force F_L, the cell length L_c and the inclination angle θ_c are used to characterize the flow dynamics of the tethered cell. L_c is the distance from the tether point to the furthest point on the membrane, which is used to represent the tether length. θ_c is the angle between L_c and the x-axis, Fig. 1b. For simplicity, L_c, θ_c, t, F_D and F_L shown in later discussions are non-dimensionalized by R, π, $1/k$, $\rho_0 k^2 R^4$ and $\rho_0 k^2 R^4$, respectively. Parameter values used in this study are listed in Table 1. From the data in Table 1, the ranges of the dimensionless parameters used in this study can be obtained as Re = 0.005 – 0.2, G = 0.02 – 0.8, $\lambda_{\mu 1}$ = 500 – 5000 and $\lambda_{\mu 2}$ = 5000 – 50,000.

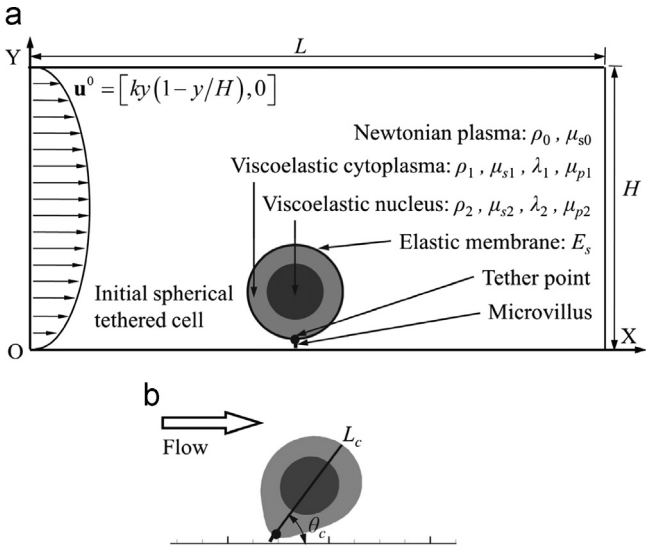

Fig. 1. Schematic diagram of a tethered cell under shear flow. (a) A cell is tethered by a microvillus on cell membrane and is subject to a parabolic shear flow. The cell is modeled as a viscoelastic compound drop (cytoplasm and nucleus) surrounded by an elastic membrane (cell membrane). (b) Parameters of the tethered cell, including the cell length L_c and the inclination angle θ_c.

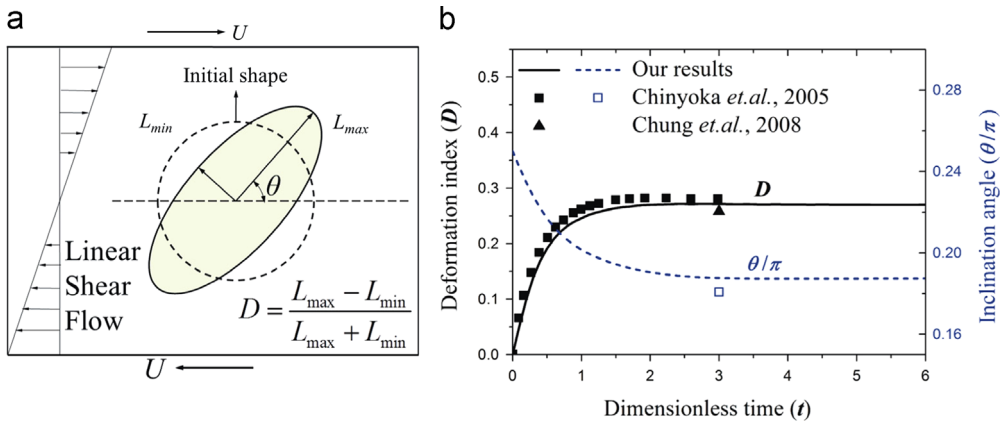

Fig. 2. Validation of our CFD code. (a) The mathematical model is validated by evaluating the deformation of a cell without a nucleus in a linear shear flow. (b) The transient deformation of a non-Newtonian drop (deformation index D and inclination angle θ versus time). The solid line (for deformation index) and dash line (for inclination angle) are our results, and square (closed square for deformation index and open square for inclination angle) and triangular dots are results from studies by Chinyoka et al. (Chinyoka, 2004; Chinyoka et al., 2005) and Chung et al. (2008).

The governing equations are solved by a two-step time-split scheme (projection method) (Brown et al., 2001). Several techniques are employed to ensure the temporal accuracy, *e.g.*, the Crank–Nicholson semi-implicit technique for the diffusion term, the Adams–Bashforth method for the advection, pressure and body force term (He and Li, 2010). The standard central difference scheme is applied to spatially discretize the governing equations to ensure the spatial accuracy. To validate our model, we simulated the deformation of a cell without a nucleus in a linear shear flow, Fig. 2a. Our model gave the deformation of Newtonian capsules (composed of elastic membrane and Newtonian cytoplasm) identical to Breyiannis's (Breyiannis and Pozrikidis, 2000) within 4.6% (data was shown in our previous study, Luo et al., 2013). These results indicated the accuracy of our model for the elastic cell membrane. Besides, to validate our non-Newtonian model for the cytoplasm, we quantitatively compared our predictions on the deformation of a non-Newtonian drop with the study carried by Chinyoka et al. (Chinyoka, 2004; Chinyoka et al., 2005) and Chung et al. (2008), Fig. 2b. The discrepancy of deformation index and inclination angle was less than 3.8%. Further details and validations of this CFD code can be found in our previous studies (Bai et al., 2013; Luo et al., 2013).

3. Results and discussions

To study the flow dynamics of a tethered cell under shear flow, we simulated the movement and deformation of a tethered cell using the mathematical model developed in the previous section. The tethered cell was with $G=0.2$, $\lambda_{\mu 1}=2000$, $\lambda_{\mu 2}=10{,}000$ and nucleus/cell volume ratio $\alpha=0.2$ in a shear flow with shear rate $k=800\ s^{-1}$, Fig. 3. After the flow began, the cell pivoted around the tether point in the flow direction (Fig. 3a) due to the positive torque from the drag force F_D on the cell (Fig. 3c). Because the cell was anchored to the bottom plate, it moved closer to the wall and was prolonged in the flow direction as time lapsed, Fig. 3a. Velocity gradients above the cell and the pressure under the cell increased over time (Fig. 3d) and thus the drag force F_D and lift force F_L experienced by the cell also increased over time (Fig. 3c). This led to an increase in the negative torque from the lift force F_L. Hence, the cell pivoting around the tether point slowed down and finally stopped due to the increasing negative torque from the lift force F_L, Fig. 3c. At the initial stage after the flow started, the fluid flow surrounding the cell was not parallel to the cell membrane, see velocity field at $t=1$ in Fig. 3d. The cell was squeezed by the pushing force from surrounding fluid behind the cell and the high pressure under the cell, Fig. 3d. The cell length L_c increased from 2 to 2.15 and the inclination angle θ_c decreased from 0.5 to 0.35 as time lapsed from $t=0$ to 1, Fig. 3b. As time lapsed to $t=2.5$, the fluid flow surrounding the cell gradually turned to be parallel to the cell membrane, see velocity field at $t=2.5$ in Fig. 3d. The cell was prolonged by the shear stress acting on the cell. The cell length L_c increased to 2.34 and the inclination angle θ_c decreased to 0.26 at $t=2.5$. However, as time further lapsed from 2.5 to 4, the cell relaxed after high deformation (*i.e.*, the cell length L_c slightly decreased to 2.24 at $t=4$) due to the elasticity of cell membrane and the viscoelasticity of internal fluids. Hence, a maximum value of cell length L_c was presented during the deforming process of tethered cell in the parabolic shear flow. The state of cell, at which the cell length L_c reached its maximum value, was defined as the largest stretching state.

To study the effect of nucleus, nucleus/cell volume ratio α and nucleus/plasma viscosity ratio $\lambda_{\mu 2}$ on the flow dynamics of the tethered cell, we next simulated the movement and deformation of four different cells under a shear flow with $k=800\ s^{-1}$, *i.e.*, a cell without nucleus ($\alpha=0$), a cell with a nucleus of $\alpha=0.2$ and $\lambda_{\mu 2}=5000$, a cell with a nucleus of $\alpha=0.2$ and $\lambda_{\mu 2}=10{,}000$ and a cell with a nucleus of $\alpha=0.44$ and $\lambda_{\mu 2}=10{,}000$, Fig. 4. The presence of a nucleus with $\alpha=0.44$ and $\lambda_{\mu 2}=10{,}000$, when cytoplasm/plasma viscosity ratio $\lambda_{\mu 1}$ was 500, led to a decrease of 33.8% in the maximum cell length L_{cm} and an increase of 152% in the inclination angle θ_{cm} at the largest stretching state compared to those of a cell without nucleus ($\alpha=0$), Fig. 4a and b. It indicated that the presence of a nucleus, which had higher viscosity than cytoplasm, significantly reduced cell deformation, Fig. 4c. The smaller deformation induced by the presence of a nucleus resulted in larger hydrodynamic forces on the tethered cell, Fig. 4d and e. Wiggles in both the drag and lift forces were observed, which is similar to the observation for an adherent monocyte under flow presented by Khismatullin and Truskey (2004). The wiggles are probably due to a combination of hydrodynamic interaction between the largely deformed cell membrane and the consequent effect that the deformed shapes have on the velocity field inside and around the cell. The drag force F_{Dm} and the lift force F_{Lm} at the largest stretching state acting on the cell with a nucleus of $\alpha=0.44$ and $\lambda_{\mu 2}=10{,}000$ were larger by 113% and 43.6% respectively than those of a cell without nucleus ($\alpha=0$), Fig. 4d and e. Due to the larger hydrodynamic forces, the cell with a nucleus reached the largest stretching state faster than the cell without nucleus. The presence of a nucleus with $\alpha=0.44$ and $\lambda_{\mu 2}=10{,}000$ resulted in a decrease of 70.8% in t_m for cells to reach the largest stretching state. Besides, as $\lambda_{\mu 2}$ was increased from 5000 to 10,000 for $\alpha=0.2$, F_{Dm} and F_{Lm} increased by 40.8% and 20.9% respectively.

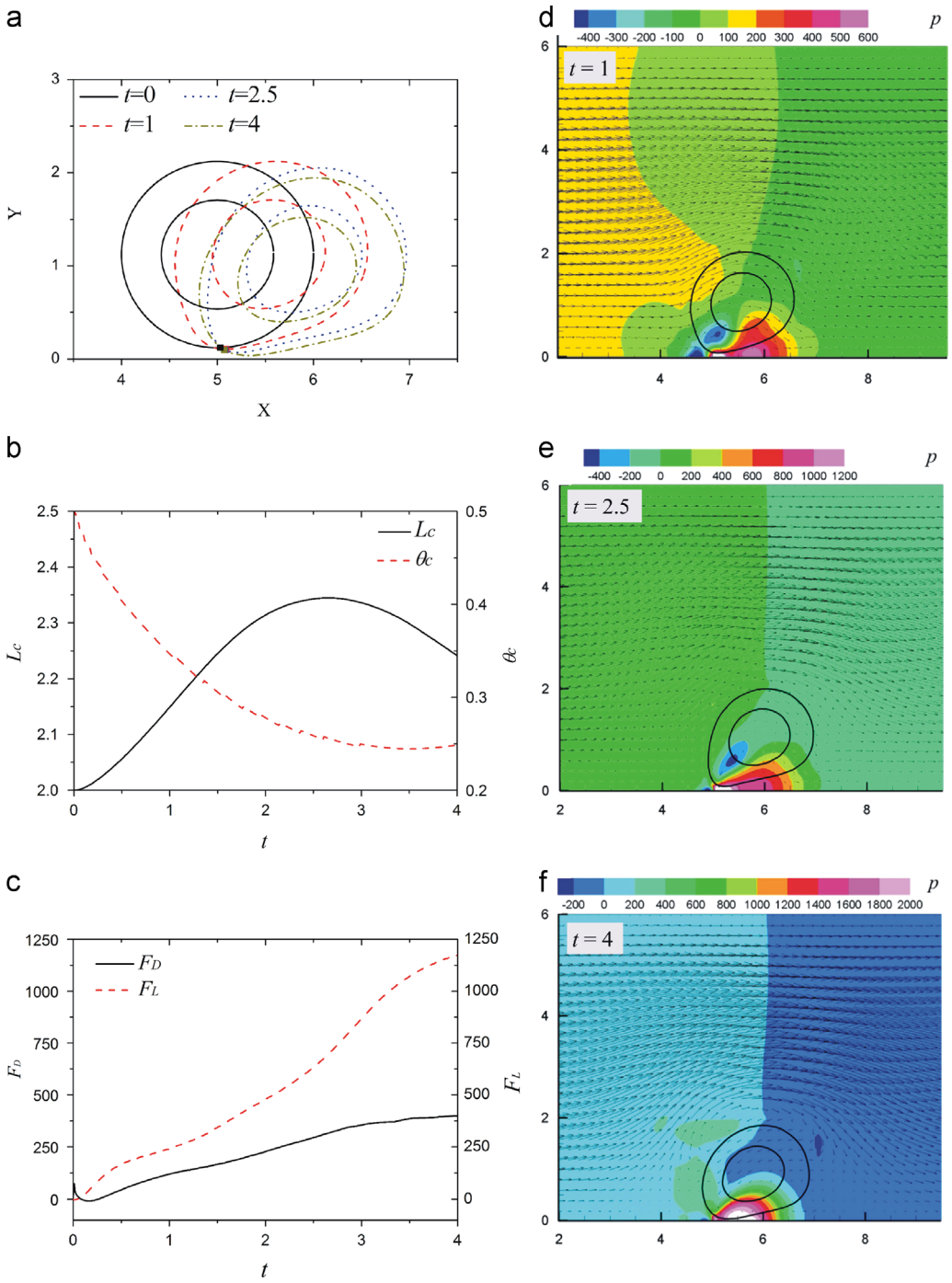

Fig. 3. Flow dynamics of a tethered cell under shear flow when $k=800\ s^{-1}$, $G=0.2$, $\lambda_{\mu 1}=2000$, $\lambda_{\mu 2}=10{,}000$ and $\alpha=0.2$. (a) Cell shape at different time points. (b) Cell length L_c and inclination angle θ_c were plotted as a function of dimensionless time t. (c) Drag force F_D and lift force F_L acting on the cell versus time. (d)–(f) Velocity vector and pressure field inside and around the cell at different times.

As α was increased from 0.2 to 0.44 for $\lambda_{\mu 2}=10{,}000$, F_{Dm} and F_{Lm} increased by 3.8% and 23.0% respectively, Fig. 4d and e. It indicated that increasing nucleus/cell volume ratio α and nucleus/plasma viscosity ratio $\lambda_{\mu 2}$ enhanced the effect of nucleus on the flow dynamics of the tethered cell.

To study the effect of cytoplasmic viscosity on the flow dynamics of the tethered cell, simulations on the movement and deformation of cells with cytoplasm/plasma viscosity ratio $\lambda_{\mu 1}$ ranging from 500 to 5000 were presented, Fig. 5. The shape of cells at the largest stretching state showed that cell elongation decreased with increasing cytoplasm/plasma viscosity ratio, Fig. 5d, which indicated higher resistance of a fluid (*i.e.*, cytoplasm) to the deformation. For the cell without nucleus ($\alpha=0$), as $\lambda_{\mu 1}$ was increased from 500 to 5000, the maximum cell length L_{cm} decreased from 3.46 to 2.34 and the inclination angle θ_{cm} increased from 0.11 to 0.25, Fig. 5b. Due to decreasing cell deformation, the hydrodynamic forces experienced by the tethered cell significantly increased with increasing $\lambda_{\mu 1}$ (from 500 to 5000), *i.e.*, the drag force F_{Dm} increased 293% and the lift force F_{Lm} increased 136%, Fig. 5c. Thus, t_m significantly decreased from 7.54 to 3.12 as $\lambda_{\mu 1}$ was increased from 500 to 5000, Fig. 5a. For the cell with a nucleus, cytoplasmic viscosity also had significant effects on

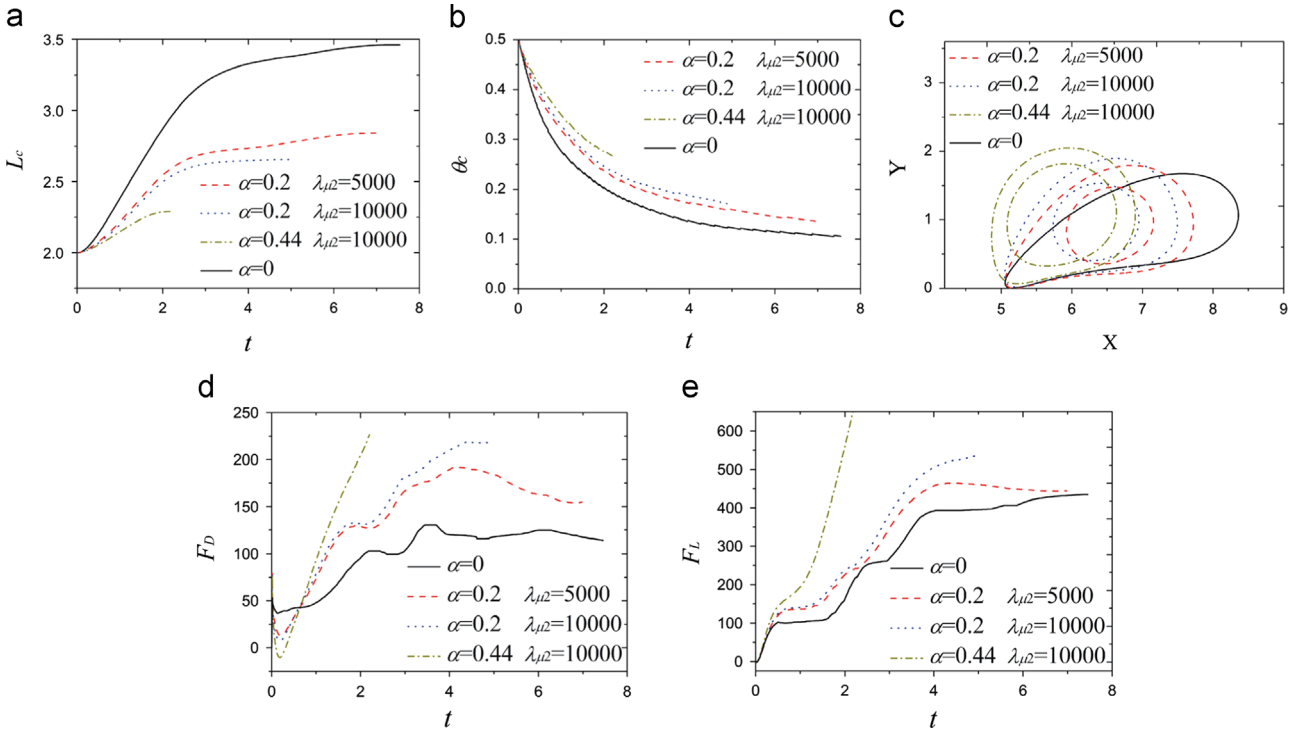

Fig. 4. Effects of nucleus, nucleus/cell volume ratio and nucleus/plasma viscosity ratio on the flow dynamics of a tethered cell. (a) Temporal evolutions of the cell length L_c and (b) the inclination angle θ_c for four different cells. (c) Cell contours when the cell length reached its maximum value for each cell. (d) and (e) Temporal evolution of the drag force F_D and the lift force F_L experienced by each cell. All the curves in (a), (b), (d) and (e) are ended at time points when the cell length reached the largest value.

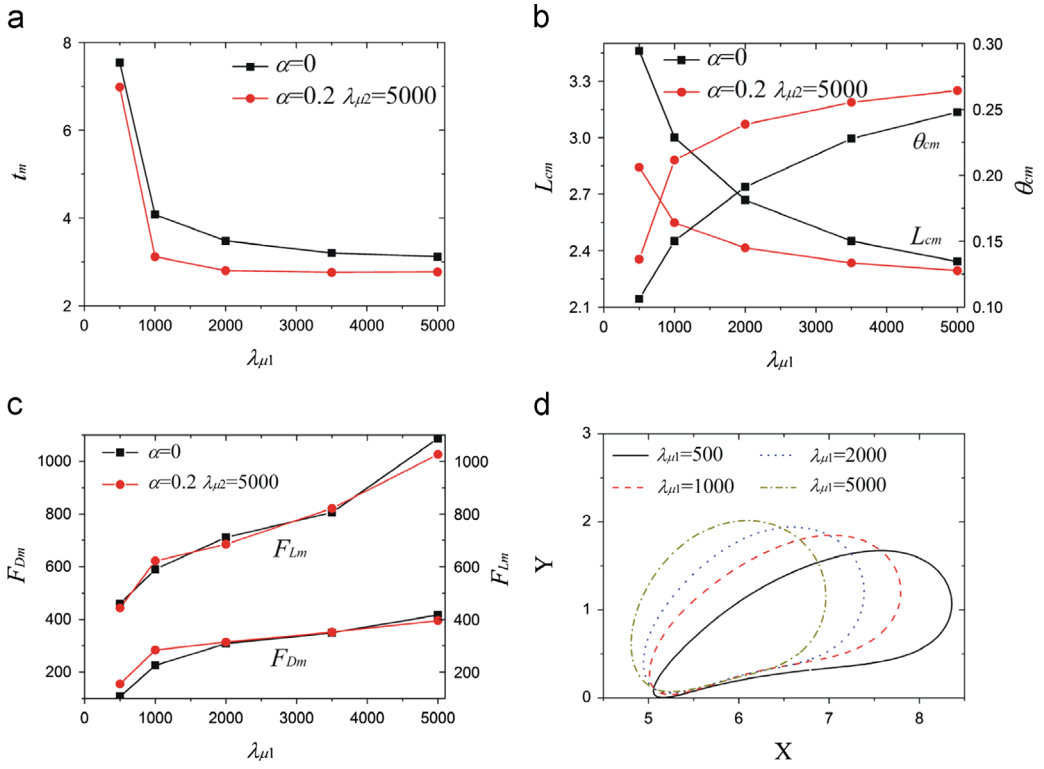

Fig. 5. Effects of cytoplasm/plasma viscosity ratio on the flow dynamics of a tethered cell. (a) The plot of the time t_m for the tethered cell to reach the longest length as a function of cytoplasm/plasma viscosity ratio. (b) The plot of the cell length L_{cm} and inclination angle θ_{cm} of cells at the largest stretching state as functions of cytoplasm/plasma viscosity ratio. (c) The plot of the drag force F_{Dm} and lift force F_{Lm} acting on the cells at the largest stretching state as functions of cytoplasm/plasma viscosity ratio. (d) Cell contours when the cell length reached its maximum value for nucleus-free cells with different cytoplasm/plasma viscosity ratios.

the flow dynamics of the tethered cell. A 10-fold increase in $\lambda_{\mu 1}$ for a cell with a nucleus of $\alpha=0.2$ and $\lambda_{\mu 2}=5000$ led to a decrease of 19.3% in the cell length L_{cm} and an increase of 93.9%, 155% and 131% in the inclination angle θ_{cm}, the drag force F_{Dm} and the lift force F_{Lm} respectively, Fig. 5a–c. However, as $\lambda_{\mu 1}$ was increased from 500 to 5000, the cell length L_{cm} decreased by 19.3% for the

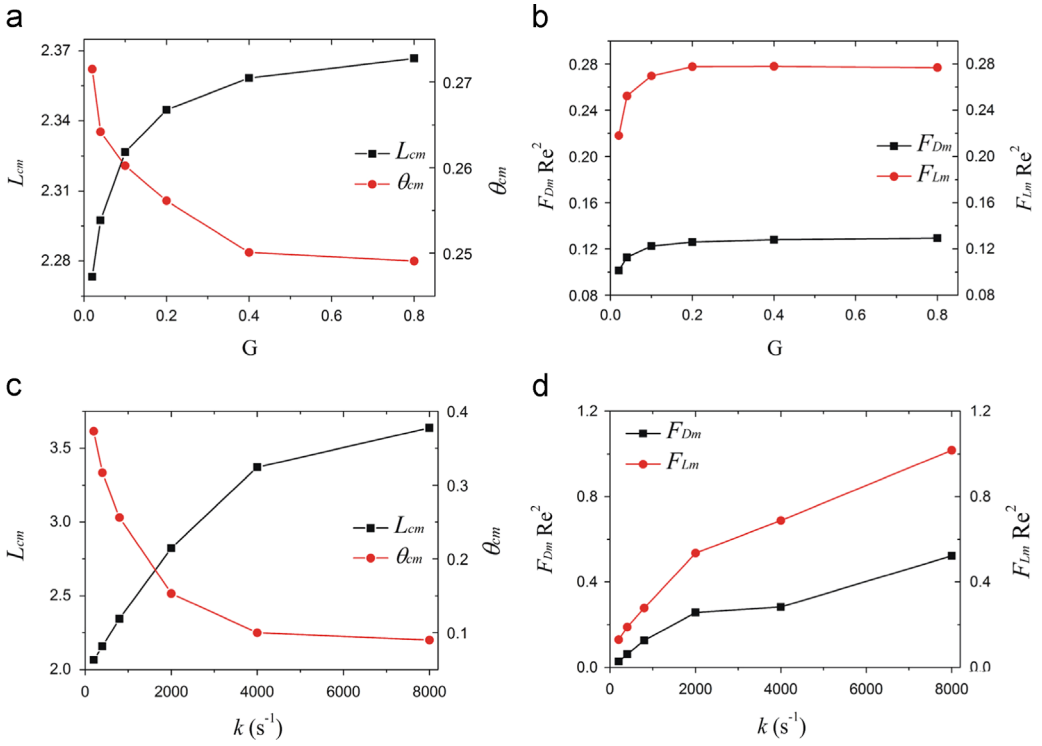

Fig. 6. Effects of membrane stiffness and shear rate on flow dynamics of a tethered cell. (a) The plot of cell length L_{cm} and inclination angle θ_{cm} of the cells at the largest stretching state as a function of dimensionless membrane stiffness. (b) Drag force F_{Dm} and lift force F_{Lm} acting on the cells at the largest stretching state as a function of dimensionless membrane stiffness. (c) The plot of cell length L_{cm} and inclination angle θ_{cm} of the cells at the largest stretching state as a function of the shear rate. (d) Drag force F_{Dm} and lift force F_{Lm} acting on the cells at the largest stretching state as a function of the shear rate. Using Re to multiply the forces is to eliminate k in the formula of the dimensionless forces.

cell with a nucleus of $\alpha=0.2$ and $\lambda_{\mu 2}=5000$, which was lower than 32.3% for the cell without nucleus ($\alpha=0$), Fig. 5b. It demonstrated that the presence of a nucleus reduced the effect of cytoplasmic viscosity on the flow dynamics of the tethered cell.

To examine effects of the membrane stiffness and shear rate on the flow dynamics of the tethered cell, we simulated the movement and deformation of cells (with the dimensionless membrane stiffness G varying from 0.02 to 0.8) in shear flows with different shear rates ($k=200$–$8000\ s^{-1}$), Fig. 6. To appropriately obtain the effect of the shear rate k on the forces, k is eliminated from the formula of the dimensionless forces by multiplying Re. The dimensionless membrane stiffness G had no significant effect on tethered cell dynamics, especially when it varied at larger values from 0.2 to 0.8, Fig. 6a and b. The cell length L_{cm} increased by 3.1% and the inclination angle θ_{cm} decreased by 5.7% as G was increased from 0.02 to 0.2, and L_{cm} increased by 0.9% and θ_{cm} decreased by 2.8% as G was increased from 0.2 to 0.8. In addition, a 40-fold increase in G only resulted in an about 1.3-fold increase in the drag force F_{Dm} and an about 1.3-fold increase in the lift force F_{Lm}. These results indicated that tethered cell dynamics were mainly affected by intracellular fluids (*i.e.*, cytoplasm and nucleus) instead of the cell membrane. The shear rate was indicated to significantly affect the flow dynamics of the tethered cell, Fig. 6c and d, which is consistent with previous experimental observations. As the shear rate was increased from 200 to $8000\ s^{-1}$, the cell length L_{cm} significantly increased from 2.07 to 3.64 and the inclination angle θ_{cm} sharply decreased from 0.37 to 0.09, Fig. 6c. Besides, the drag force F_{Dm} and lift force F_{Lm} depended nonlinearly on the shear rate: a 40-fold increase of the shear rate resulted in an about 18.3-fold increase in F_{Dm} and an about 7.7-fold increase in F_{Lm}, Fig. 6d.

In summary, we developed a two-dimensional mathematical model to investigate the flow dynamics of nucleated cells tethered under shear flow. According to our simulations, the cell length L_c significantly increased with increasing shear rate, which is qualitatively consistent with previous experimental observations (Schmidtke and Diamond, 2000; Dopheide et al., 2002; Ramachandran et al., 2004). The cell pivoted around the tether point and moved closer to the bottom plate with time, which may strengthen the adhesion of the cell to the bottom plate. This result may partly explain the observed phenomenon in experiments that cell tether formation stabilized cell rolling (Ramachandran et al., 2004). Our results showed that a variation in cytoplasmic viscosity ($\lambda_{\mu 1}=500-5000$) led to a large variation in cell tether length (from $0.34R$ to $1.46R$). This result is in parallel with the experimental observation of large variations in leukocyte tether length from 1 to 25 μm (about $0.16R$ to $4.16R$) (Schmidtke and Diamond, 2000). Besides, the presence of a nucleus, nucleus/cell volume ratio and nucleus/plasma viscosity ratio were found to significantly affect tethered cell dynamics. This becomes another important reason besides initial cell shape (cell aspect ratio) (Berry et al., 2011) for distinct characteristics of tethered cell dynamics (*e.g.*, tether length) between different blood components (*e.g.*, leukocytes and platelets) (Schmidtke and Diamond, 2000; Dopheide et al., 2002; Ramachandran et al., 2004). Our mathematical model captured the general features of tethered cell dynamics under shear flow, which are consistent with experimental observations.

Cell tethers can form before or during cell rolling, and were found to stabilize cell rolling, which was demonstrated in the experimental study by Ramachandran et al. (2004) and in the three-dimensional numerical study by Khismatullin and Truskey (2012). In Khismatullin's study (Khismatullin and Truskey, 2012), the leukocyte cytoplasmic viscosity played a critical role in leukocyte rolling on an adhesive substrate. In this study, we found that the presence of a nucleus, increasing nucleus/cell volume ratio and nucleus/plasma viscosity ratio significantly affected cell tether dynamics, which is an important reason for distinct

characteristics between leukocyte tethers and platelet tethers. The model presented in this study included both the elasticity of cell membrane and the viscosity of cytoplasm and nucleus, which was not presented in previous models (Khismatullin and Truskey, 2012; Pappu and Bagchi, 2008; Pappu et al., 2008). Logical extensions of this model to a three-dimensional model and using more biologically relevant descriptions for the elasticity of cell membrane and the viscoelasticity of internal fluids would be helpful to more accurately study the underlying mechanisms of tethered cell dynamics under shear flow. Besides, tethers of leukocytes and platelets observed in experiments are long thin cylinders pulled out from cell membrane, while this tether formation process was not captured in our model. It is a deficiency of such models (Berry et al., 2011), which only included the elastic property of cell membrane while not the viscous property. The viscosity of cell membrane was demonstrated to be important in the formation of cell tethers (King et al., 2005; Jauffred et al., 2007; Schmitz et al., 2008). Therefore, to include the membrane viscosity into our model is essential to further study the dynamics of cell tethers.

4. Conclusion

A two-dimensional mathematical model was developed to investigate the effects of the presence of a nucleus, nucleus/cell volume ratio, nucleus/plasma viscosity ratio and cytoplasm/plasma viscosity ratio on the flow dynamics of a nucleated cell tethered under shear flow, *e.g.*, the cell length, the inclination angle, the drag force and lift force acting on the tethered cell. Our major findings include (1) the cell was elongated by the surrounding flow and pivoted around the tether point toward the bottom plate, and a maximum value of the cell length was presented as the cell relaxed after large deformation; (2) the presence of a nucleus, increasing nucleus/cell volume ratio and nucleus/plasma viscosity ratio decreased the maximum cell length and increased the inclination angle, the drag and lift forces acting on the tethered cell; (3) cell membrane elasticity had relatively small effect but cytoplasm/plasma viscosity ratio had significant effects on the flow dynamics of tethered cell. Our study provides new insights into the flow dynamics of tethered cells under shear flow and could help to further understand the role of cell tether on cell adhesion related bioprocesses and microfluidics, *e.g.*, regulating cell adhesion strength, stabilization of cell rolling, and clot formation inside blood vessels.

Nomenclature

De	Deborah number, $De=\lambda k$
E_s	elastic modulus of cell membranes, μN/m
$\mathbf{F}$	body force in Eq. (2)
$\boldsymbol{F}_{hy}$	vector of hydrodynamic forces acting on the tethered cell
F_D	drag force acting on the tethered cell, N
F_L	lift force acting on the tethered cell, N
G	dimensionless stiffness of cell membrane, $G=\mu_0 kR/E_s$
h	Eulerian grid size
H	channel height as illustrated in Fig. 1, μm
$\mathbf{I}$	unit tensor in Eq. (2)
I	indicator function in Eq. (6)
k	bulk shear rate of channel flow, 1/s
L_c, θ_c	cell length and inclination angle as illustrated in Fig. 1b
L	channel length as illustrated in Fig. 1, μm
$\mathbf{n}$	unit outward normal vector to cell membrane
p	pressure, Pa
R	cell radius, μm
Re	Reynolds number, $Re=\rho_0 kR^2/\mu_0$
$\mathbf{T}_p$	viscoelastic stress in Eq. (2)
T_e	membrane tension in Eq. (4), N
t	time, s
$\mathbf{u}$	vector of velocity in Eq. (2)
$\boldsymbol{x}$	vector of position at Eulerian grid
$\boldsymbol{x}'$	vector of position at Lagrangian grid

Greek letters

ρ_0, ρ_1, ρ_2	density of surrounding fluid, cytoplasma and nucleus respectively, kg/m^3
μ_0, μ_1, μ_2	viscosity of surrounding fluid, cytoplasma and nucleus respectively, Pa s
μ_p, μ_s	polymeric viscosity and solvent viscosity of viscoelastic fluids respectively, Pa s
ε	principal stretch ratio
α	nucleus/cell volume ratio
$\lambda_{\mu 1}$, $\lambda_{\mu 2}$	cytoplasm/plasma viscosity ratio and nucleus/plasma viscosity ratio respectively
λ_1, λ_2	relaxation time of cytoplasm and nucleus respectively, s

Acknowledgments

This work was supported by the Specialized Research Fund for the Doctoral Program of Higher Education of China (20110201110029). This research was partially supported by the National Natural Science Foundation of China. Utkan Demirci acknowledges that this material is based in part upon work supported by the National Science Foundation under NSF CAREER Award numbers 1150733 and NIH R01 EB015776.

References

Bagchi, P., 2007. Mesoscale simulation of blood flow in small vessels. Biophys. J. 92, 1858–1877.
Bagchi, P., Johnson, P.C., Popel, A.S., 2005. Computational fluid dynamic simulation of aggregation of deformable cells in a shear flow. J. Biomech. Eng. – Trans. ASME 127, 1070–1080.
Bai, B.F., Luo, Z.Y., Lu, T.J., et al., 2013. Numerical simulation of cell adhesion and detachment in microfluidics. J. Mech. Med. Biol. 13, 1350002.
Barthes-Biesel, D., Diaz, A., Dhenin, E., 2002. Effect of constitutive laws for two-dimensional membranes on flow-induced capsule deformation. J. Fluid Mech. 460, 211–222.
Berry, J.D., Carberry, J., Thompson, M.C., 2011. Flow dynamics of a tethered elastic capsule. Phys. Fluids 23, 021901.
Breyiannis, G., Pozrikidis, C., 2000. Simple shear flow of suspensions of elastic capsules. Theor. Comput. Fluid Dyn. 13, 327–347.
Brown, D.L., Cortez, R., Minion, M.L., 2001. Accurate projection methods for the incompressible Navier–Stokes equations. J. Comput. Phys. 168, 464–499.
Chinyoka, T., 2004. Numerical Simulation of Stratified Flows and Droplet Deformation in Two-dimensional Shear Flow of Newtonian and Viscoelastic Fluids. Virginia Polytechnic Institute and State University, Virginia.
Chinyoka, T., Renardy, Y.Y., Renardy, A., et al., 2005. Two-dimensional study of drop deformation under simple shear for oldroyd-b liquids. J. Non-Newton. Fluid Mech. 130, 45–56.
Chung, C., Hulsen, M.A., Kim, J.M., et al., 2008. Numerical study on the effect of viscoelasticity on drop deformation in simple shear and 5:1:5 planar contraction/expansion microchannel. J. Non-Newton. Fluid Mech. 155, 80–93.
Dopheide, S.M., Maxwell, M.J., Jackson, S.P., 2002. Shear-dependent tether formation during platelet translocation on von willebrand factor. Blood 99, 159–167.
Geissmann, F., Jung, S., Littman, D.R., 2003. Blood monocytes consist of two principal subsets with distinct migratory properties. Immunity 19, 71–82.
Girdhar, G., Shao, J.Y., 2007. Simultaneous tether extraction from endothelial cells and leukocytes: observation, mechanics, and significance. Biophys. J. 93, 4041–4052.
Gurkan, U.A., Tasoglu, S., Akkaynak, D., et al., 2012. Smart interface materials integrated with microfluidics for on-demand local capture and release of cells. Adv. Healthc. Mater. 1, 661–668.
He, Y.N., Li, J., 2010. Numerical implementation of the crank-nicolson/adams-bashforth scheme for the time-dependent Navier–Stokes equations. Int. J. Numer. Methods Fluids 62, 647–659.

Heinrich, V., Leung, A., Evans, E., 2005. Nano- to microscale dynamics of p-selectin detachment from leukocyte interfaces. Ii. Tether flow terminated by p-selectin dissociation from psgl-1. Biophys. J. 88, 2299–2308.
Jadhav, S., Eggleton, C.D., Konstantopoulos, K., 2005. A 3-d computational model predicts that cell deformation affects selectin-mediated leukocyte rolling. Biophys. J. 88, 96–104.
Jauffred, L., Callisen, T.H., Oddershede, L.B., 2007. Visco-elastic membrane tethers extracted from escherichia coli by optical tweezers. Biophys. J. 93, 4068–4075.
Khismatullin, D.B., Truskey, G.A., 2004. A 3d numerical study of the effect of channel height on leukocyte deformation and adhesion in parallel-plate flow chambers. Microvasc. Res. 68, 188–202.
Khismatullin, D.B., Truskey, G.A., 2005. Three-dimensional numerical simulation of receptor-mediated leukocyte adhesion to surfaces: effects of cell deformability and viscoelasticity. Phys. Fluids 17, 21.
Khismatullin, D.B., Truskey, G.A., 2012. Leukocyte rolling on p-selectin: a three-dimensional numerical study of the effect of cytoplasmic viscosity. Biophys. J. 102, 1757–1766.
King, M.R., Heinrich, V., Evans, E., et al., 2005. Nano-to-micro scale dynamics of p-selectin detachment from leukocyte interfaces. Iii. Numerical simulation of tethering under flow. Biophys. J. 88, 1676–1683.
Luo, Z.Y., Wang, S.Q., He, L., et al., 2013. Front tracking simulation of cell detachment dynamic mechanism in microfluidics. Chem. Eng. Sci. 97, 394–405.
Luo, Z.Y., Xu, F., Lu, T.J., et al., 2011a. Direct numerical simulation of detachment of single captured leukocyte under different flow conditions. J. Mech. Med. Biol. 11, 273–284.
Luo, Z.Y., Xu, F., Lu, T.J., et al., 2011b. Direct numerical simulation of single leukocyte deformation in microchannel flow for disease diagnosis. J. Med. Syst. 35, 869–876.
Muradoglu, M., Tasoglu, S., 2010. A front-tracking method for computational modeling of impact and spreading of viscous droplets on solid walls. Comput. Fluids 39, 615–625.
N'Dri, N.A., Shyy, W., Tran-Son-Tay, R., 2003. Computational modeling of cell adhesion and movement using a continuum-kinetics approach. Biophys. J. 85, 2273–2286.
Pappu, V., Bagchi, P., 2008. 3d computational modeling and simulation of leukocyte rolling adhesion and deformation. Comput. Biol. Med. 38, 738–753.
Pappu, V., Doddi, S.K., Bagchi, P., 2008. A computational study of leukocyte adhesion and its effect on flow pattern in microvessels. J. Theor. Biol. 254, 483–498.
Peskin, C.S., 1977. Numerical analysis of blood flow in the heart. J. Comput. Phys. 25, 220–252.
Popel, A.S., Johnson, P.C., 2005. Microcirculation and hemorheology. Annu. Rev. Fluid Mech. 37, 43–69.
Pospieszalska, M.K., Ley, K., 2009. Dynamics of microvillus extension and tether formation in rolling leukocytes. Cell. Mol. Bioeng. 2, 207–217.
Ramachandran, V., Williams, M., Yago, T., et al., 2004. Dynamic alterations of membrane tethers stabilize leukocyte rolling on p-selectin. Proc. Natl. Acad. Sci. USA 101, 13519–13524.
Rizvi, I., Gurkan, U.A., Tasoglu, S., et al., 2013. Flow induces epithelial–mesenchymal transition, cellular heterogeneity and biomarker modulation in 3d ovarian cancer nodules. Proc. Natl. Acad. Sci. USA 110, E1974–E1983.
Sarkar, K., Schowalter, W.R., 2000. Deformation of a two-dimensional viscoelastic drop at non-zero reynolds number in time-periodic extensional flows. J. Non-Newton. Fluid Mech. 95, 315–342.
Schmid-Schonbein, G.W., Shih, Y.Y., Chien, S., 1980. Morphometry of human leukocytes. Blood 56, 866–875.
Schmidtke, D.W., Diamond, S.L., 2000. Direct observation of membrane tethers formed during neutrophil attachment to platelets or p-selectin under physiological flow. J. Cell Biol. 149, 719–729.
Schmitz, J., Benoit, M., Gottschalk, K.E., 2008. The viscoelasticity of membrane tethers and its importance for cell adhesion. Biophys. J. 95, 1448–1459.
Squires, T.M., Quake, S.R., 2005. Microfluidics: fluid physics at the nanoliter scale. Rev. Mod. Phys. 77, 977–1026.
Stone, H.A., Kim, S., 2001. Microfluidics: basic issues, applications, and challenges. AIChE J. 47, 1250–1254.
Tasoglu, S., Kaynak, G., Szeri, A.J., et al., 2010. Impact of a compound droplet on a flat surface: a model for single cell epitaxy. Phys. Fluids 22, 082103.
Tasoglu, S., Demirci, U., Muradoglu, M., 2008. The effect of soluble surfactant on the transient motion of a buoyancy-driven bubble. Phys. Fluids 20, 040805.
Tasoglu, S., Gurkan, U.A., Wang, S., et al., 2013. Manipulating biological agents and cells in microscale volumes for applications in medicine. Chem. Soc. Rev. 42, 5788–5808.
Tasoglu, S., Safaee, H., Zhang, X., et al., 2013. Exhaustion of racing sperm in nature-mimicking microfluidic channels during sorting. Small 9, 3374–3384. http://dx.doi.org/10.1002/smll.201300020.
Tasoglu, S., Park, S.C., Peters, J.J., Katz, D.F., Szeri, A.J., 2011. The consequences of yield stress on deployment of a non-Newtonian anti-HIV microbicide gel. J. Non-Newton. Fluid Mech. 166, 1116–1122.
Tasoglu, S., Katz, D.F., Szeri, A.J., 2012. Transient spreading and swelling behavior of a gel deploying an anti-HIV microbicide. J. Non-Newton. Fluid Mech. 187-188, 36–42.
Tryggvason, G., Bunner, B., Esmaeeli, A., et al., 2001. A front-tracking method for the computations of multiphase flow. J. Comput. Phys. 169, 708–759.
Unverdi, S.O., Tryggvason, G., 1992. A front-tracking method for viscous, incompressible, multi-fluid flows. J. Comput. Phys. 100, 25–37.
Yago, T., Zarnitsyna, V.I., Klopocki, A.G., et al., 2007. Transport governs flow-enhanced cell tethering through l-selectin at threshold shear. Biophys. J. 92, 330–342.
Yu, Y., Shao, J.Y., 2007. Simultaneous tether extraction contributes to neutrophil rolling stabilization: a model study. Biophys. J. 92, 418–429.